Analysis and Evaluation of the NASA/JPL TOPSAR Across-track Interferometric SAR System

S. N. MADSEN, J. MARTIN, AND H. A. ZEBKER

Jet Propulsion Laboratory, California Institute of Technology

ABSTRACT

We have evaluated the accuracy of digital elevation models (DEMs) generated by the JPL/NASA TOPSAR synthetic aperture radar interferometer instrument by acquiring topographic data in the summer of 1992 over the National Training Center, Ft. Irwin, California, a desert area with significant relief and varied terrain, and comparing the measurements to a very accurate digital elevation model derived for this area by the U.S. Army Topographic Engineering Center (TEC). Fiducial comer reflectors were deployed in the area, and their locations were determined to cm accuracy by the Defense Mapping Agency (DMA) using differential GPS techniques. DEMs generated from the acquired radar data were rotated and translated to precisely overlay the reference DEM, allowing an in-depth analysis of the achieved height accuracy.

We present here a detailed description of horizontal and vertical errors and their characteristics. The standard deviation measured over a 5.6 by 7 km area was approximately 2 m, the corresponding figures for relatively flat areas were in the 1 to 2 meter range and for mountainous areas in the 2 to 3 meter range, which are consistent with theoretical expectations. We also discuss key factors that presently limit the system performance.

Keywords: SAR interferometry, topographic mapping, 3-D imaging radar

---

Version 1.2, October 14, 1993,9:55

Submitted to the IEEE transactions for Geoscience and Remote Sensing on 93/09/DD

Please address any communication to:

Søren Nørvang Madsen, MS 300-235

Jet Propulsion Laboratory

4800 Oak Grove Dr.

Pasadena, CA 91109

Phone: (818) 3548353

Fax: (818) 3935285

E-mail: soren@tivoli.jpl.nasa.gov

1. INTRODUCTION

Radar mapping utilizing interferometric principles was first applied in the late 1960's and early 1970's to earth-based observations of Venus and the moon, [1--4]. At this time it was also shown experimentally by Graham [5] that an interference pattern which contains information about the target topography is obtained by coherent addition of the receiver signals from two spatially separated SAR antennas.

We have studied topographic mapping using interferometric SAR for several years. Zebker and Goldstein [6] demonstrated that two interferometric channels could be individually processed to complex images which were combined to give a complex interferogram with phase information which is directly related to the surface topography. Goldstein et al. [7] then developed a phase unwrapping technique to produce a unique phase difference between any two points in the interferograrn, which is not the case in the complex data as the phase differences are only known modulo 2π. More recently Zebker et al. [8] reported on the JPL TOPSAR system, a C-band SAR across-track interferometer, and Madsen et al. [9] described an integrated topographic processor which includes SAR data compression algorithms, motion compensation algorithms, phase unwrapping and absolute phase determination, as well as regrinding algorithms. The absolute phase is required to establish a direct relationship between the unwrapped phase and the slant range difference from the target to the two antennas [10]. An initial evaluation of TOPSAR accuracy was completed in 1991, and the system performance was shown to be compatible with or better than standard United States Geological Survey (USGS) 7,5-minute digital elevation models [9], Based on our experiences from the 1991 evaluation campaign an experiment was planned to further study the performance and limitations of the TOPSAR system, In 1992 we acquired TOPSAR data over the National Training Center, Ft. Irwin, California, a desert area with significant relief. The range of height in the target area was from 930 m to 1488 m, and the height standard deviation was 150 m. Here we describe the methodology of that experiment as well as the results wc obtained with respect to both horizontal and vertical accuracies. In addition, we have attempted to identify the most important limitations and error sources for this technique.

We have organized this paper as follows. In section 2 we will provide a brief description and estimated performance of the JPL TOPSAR radar system. Section 3 describes the details of the experiment which

is the core of this report. The results of the experiment are presented in section 4 and we discuss the most important limitations and error sources in section 5. Section 6 summarizes our conclusions.

2. THE TOPSAR RADAR SYSTEM

The TOPSAR radar system has been described previously by Zebker et al. [8] and therefore only the most significant parameters will be summarized here. The TOPSAR system uses the C-band channels of the JPL/NASA AIRSAR DC-8 airborne synthetic aperture radar system. The basic TOPSAR parameters in the configuration flown in 1992 are shown in Table. 1.

TOPSAR utilizes two antennas which arc flush mounted on the left side of the DC-8. The antennas are mounted at the same along-track position with a separation in the cross-track plane of 2.5 m. The boresights of the antennas are depressed 45° with respect to horizontal. One antenna is used for transmission and the signals received by both antennas arc recorded independently. The slant range resolution of the system is limited by the system bandwidth (40 MHz) to 3.75 m and the slant range swath width after range compression is 4.4 km. Data can also be acquired at 7.5 m resolution, in which case the swath after range compression is more than doubled.

The aircraft is equipped with three navigation systems. The digital avionics data system (DADS) includes the aircraft inertial navigation system, a barometric altimeter, a radar altimeter, as well as a number of other navigation systems allowing the system to be updated in flight. The second system is a global positioning system (GPS), and the third is the radar inertial navigation system (LASEREF). The DADS and GPS data are quite accurate (GPS accuracy typically 25–75 m), but are only updated approximately once per second. The LASEREF, on the other hand, provides accelerations and attitudes at a 50 Hz rate. However, it is not locked to other systems and biases in position, elevation and velocities tend to increase with time. To obtain low drift with time as well as high up-date rate we combined the different data sets as described earlier [9].

The TOPSAR geometry is depicted in Fig. 1, where (after [8]), the interferometer baseline of length B is aligned at an a with respect to horizontal, the aircraft is at height h and distance ρ from the target, the look angle is θ, and the target is at local altitude z , and the local slope is γ. A detailed discussion of error sources will be presented in section 5 below. We may, however, roughly estimate the expected performance given the system configuration as follows. The principal contributions to height uncertainty σ_h from phase noise σ_ϕ and baseline orientation (roll) error σ_α were derived by Zebker et al. [8] and Rodriguez and Martin[11]

$$\sigma_{h,\phi} = \frac{\lambda\rho}{2\pi B}\frac{\sin\theta}{\cos(\alpha - 0)}\,\sigma_{\phi} = \frac{\lambda\rho}{2\pi B_{\perp}}\sin\theta\,\sigma_{\phi} \quad (1)$$

($B_{\perp} = B\cos(\alpha - O)$ is the perpendicular baseline), and

$$\sigma_{h,\alpha} = p\sin\theta\,\sigma_{\alpha} \quad (2)$$

At the center of our swath the system nominally exhibits a phase noise due to thermal noise of 2,4° (SNR = 13 dB) assuming 30 radar looks of a target at a normalized radar cross-section σ_0 of -15 dB, and wc obtain a height noise of 1.3 m. To this has to be added a baseline decorrelation noise (see section 5) which is on the order of 0.7 m. As will be discussed below, the contribution from long time roll bias errors can be compensated for using tie points, leaving only the contribution from higher frequency aircraft motions. Our expected height error noise at the center of swath is thus 1.5 m.

3. THE FT. IRWIN EXPERIMENT 1992

The Ft. Irwin 1992 evaluation was designed to improve on some of the deficiencies of the 1991 experiments. Sponsored by the Advanced Research projects Agency (ARPA), we collected data over the Army National Training Center (NTC), Ft. Irwin, California on July 8th, 1992. Our flight tracks were designed to intersect at an area which was being mapped very accurately by the U.S. Army's Topographic Engineering Center (TEC). Comer reflectors were deployed in the area, and their locations were determined to centimeter accuracy by the Defense Mapping Agency (DMA) using differential GPS techniques. The TEC reference provided us with a reliable and very accurate reference and the surveyed comer reflectors enabled us to co-register the radar data accurately on the reference data. The Ft. Irwin area, including the area covered by the TEC DEM, and the radar tracks are shown in Fig. 2. This figure also indicates the positions of the deployed comer reflector as solid black triangles. We deployed a total of ten 8 foot comer reflectors, four reflectors facing run 1, three reflectors each for runs 2 and 3. The UTM positions of the comer reflectors relative to WGS 84 as well as the comers of the reference DEM are given in Table 2.

The Ft. Irwin area is a desert with significant relief. Heights in the target area vary from 930 m to 1488 m above the WGS--84 ellipsoid, and the height standard deviation is 150 m. The terrain is a mixture of mountainous areas, consisting mainly of granite rocks, and flatter areas consisting primarily of alluvium. The vegetation is sparse and low and is thus of minor importance in relation to evaluating the radar DEM accuracy. The very accurate reference DEM was derived for this area by TEC using digital correlation methods on 1:20,000 scale digitized photographs. The reference DEM covered a 5.6

by 7 km area at a post (pixel) spacing of 5 m. As the standard output of the TOPSAR processor is samples at 10 m horizontal spacing, we used a subsampled version of the reference DEM also with 10 m sample spacing. The verified accuracy of the DEM (TEC checked 84 surveyed reference points) was 0.3 m with respect to WGS-84. The reference DEM is shown in color coded and shaded relief presentations in Fig. 3.

A total of 3 TOPSAR data sets were acquired consisting of two east-west opposite side mapping tracks and one north-south track. Runs 1 and 3 of the radar data were processed on the standard integrated TOPSAR processor as described previously [9]. Run 2 was a new wide swath product which was processed on a modified version of the processor, The evaluation we are presenting here will only use the standard products. An inherent property of the processor is that it determines the along-track, x, across-track, y, and vertical, z, coordinates of every single image point, and the output product is uniformly spaced in x and y. Therefore, intrinsic radar distortions such as lay-over, foreshortening, and squint distortions arc compensated. The TOPSAR processor generates data at a uniform x and y pixel spacing of 5 m, but to reduce the vertical measurement noise a post processing step is added which reduces the resolution to approximately 15 m and the pixel spacing to 10 m. A sample radar image is shown in Fig. 4, where the image brightness is proportional to the radar backscatter and the height is mapped onto a color wheel with 16 colors. Each color represents a 2 m height interval and the colors are thus repeated when the height changes by 32 m. The radar DEMs were co-registered horizontally to the TEC DEM using the comer reflectors as tie-points. The positions of the comer reflectors were determined in the 5 m radar image products and assuming a uniform distribution of the position error in the intervat ±2.5 m we would expect an rms. error of $2.5/\sqrt{3}$ = 1.4 m or 0.14 times the 10 m pixel spacing. Knowing both the radar coordinates and the UTM coordinates for the comer reflectors wc can determine the transformation from radar coordinates to UTM, and from the transformation matrix we can deduce the horizontal azimuth and range scaling errors and the skew.

We established the vertical alignment using two different approaches: 1) by removing an azimuth slope, a range slope, and a height offset based on corner reflector measurements; and 2) by removing an azimuth and a range slope and a height offset which matches the TEC DEM in a least square error sense.

After re-sampling the radar data to the reference DEM we analyzed the height errors on a pixel to pixel basis. We measured mean, standard deviation, and the standard deviation after rejection of 50 values.

4. RESULTS

The horizontal transformation wc applied was reduced to the form:

$$\begin{pmatrix} x \\ y \end{pmatrix}_{DEM} = \begin{pmatrix} \cos\theta & \sin\theta \\ -\sin\theta & \cos\theta \end{pmatrix} \begin{pmatrix} 1 & 0 \\ \gamma & 1 \end{pmatrix} \begin{pmatrix} \lambda_x & 0 \\ 0 & \lambda_y \end{pmatrix} \begin{pmatrix} x \\ y \end{pmatrix}_{TOPSAR} + \begin{pmatrix} \delta x \\ \delta y \end{pmatrix} \quad (3)$$

where θ is the rotation angle which will align the aircraft along-track axis with UTM northing, γ is the skew, λ_x is the along-track scale factor, λ_y is the across-track scale factor and $(\delta x, \delta y)^T$ is the translation required to co-align the TOPSAR DEM to the TEC DEM. From a comparison of the TOPSAR and TEC DEMs, we measured the transformation parameters shown in Table 3.

Only three corner reflectors are required to determine the horizontal transformation, and the extra reflector available for RUN 1 permitted a consistency check of the transformation. By transforming the *4* surveyed comer reflector locations to radar coordinates (x, y) we found deviations relative to the observed positions of 2.4 m in ground range and 0.8 m in azimuth. This is approximately half the resolution of the radar image before any multi-looking.

It is worth noting that due to an inconsistency in our original implementation of the program which averages the data down from the 5 m pixel spacing to the 10 m pixel spacing wc had a systematic offset of 2.5 m in both range and azimuth in early tests. This 2.5 m misalignment gave rise to a 15 to 25 % increase in the measured vertical error (see section 5). This inconsistency was corrected for the work shown in this paper. It clearly illustrates the sensitivity of the height errors to horizontal geometric fidelity and data registration,

Having determined the horizontal transformation, we determined the vertical planar offset by two methods. The first relies entirely on the corner reflector locations and heights and the second method estimates the planar offset by minimizing the errors over the whole DEM in a least mean square sense.

The parameters of the planar offset using the former approach (comer reflectors only) are given in Table 4. The table shows the azimuth (along-track) and range (across-track) tilts as well as the vertical offset. Also shown are the standard deviations of the terrain elevations in the area where the radar and the reference DEMs overlap along with the mean and standard deviation of the differences. Furthermore the table shows the number of points exceeding 5 times the standard deviation as well as the measured standard deviation when those points are not included in the statistics. Nearly all of the rejected points

were located in shadow areas on mountain slopes tilting away from the radar and the maximum error was approximately 50 m. Note that there are few rejected points and that the standard deviation is approximately the same whether they are included in the analysis or not. Also note that the standard deviation is significantly smaller for run 1 data than for run 3 data. The three comer reflectors applicable to run 3 lie nearly on a straight line oriented along-track and the range tilt is thus not very well determined. This result emphasizes the importance of well distributed fiducial points.

The inaccuracy in the tilt determination can be avoided by using the reference DEM for the vertical alignment. We therefore added a second linear function which removed the systematic height offset and the northing/casting tilts of the difference height map (radar minus reference). The difference of the radar and reference DEMs after the removal of this planar offset is shown in Table 5. This table again shows the standard deviations of the terrain elevation for the windows analyzed, the number of points in the window, the mean and standard deviations of the height difference maps, the number of points exceeding 5 sigma, and finally the standard deviation of the height difference if those points are ignored. We present the results of three analyses, for the entire area of overlap, a predominantly flat area and a mountainous area. The mountain areas were the same for both runs, but the flat area was changed to be in the same part of the swath in each case (at comparable incidence angles).

In figures 5 and 6 we show color encoded height difference maps. It is obvious that the horizontal registration is quite good as height errors are not are not systematically correlated with the orientation of the mountain s1OPCS. This is consistent with our earlier observation that the registration accuracy is on the order of the one-look resolution of the radar data (5 m in ground range, 0.8 m in azimuth). On the other hand it is also clear that the height error dots increase when the terrain slope increases, consistent with the observation that image resolution becomes an issue when the horizontal resolution times the tangent of the terrain slope is somewhat larger than the desired vertical resolution. This is the case on many mountain slopes in the Ft. Irwin area.

In figures 7 and 8 we show data from linear segments through the run 1 data shown in figure 5. The ground tracks are oriented east-west and north-south through the mountainous region in the northwest corner of the TEC DEM. At the scale of the terrain height variation the differences are barely discernible and thus we also plotted the difference between the radar and the TEC DEMs. The largest deviation (12.5 m) is found in the north-south line and it is seen to be exactly coinciding with a peak where the radar height measurement is larger than the TEC DEM measurement.

5. DISCUSSION OF ERROR SOURCES

In this section we discuss error sources and identify the dominant errors for this experiment, First we note that if terrain slopes differ from zero any horizontal error will translate into a vertical error given by

$$\sigma_{h,y} = \sigma_y \tan \gamma \qquad (4)$$

where $\sigma_{h,y}$ is the vertical error caused by a horizontal error, σ_y is the horizontal error, and y is the terrain slope. The dominant horizontal error sources and vertical error sources for our system arc listed in tables 6 and 7, respectively,

High frequency errors introduced by thermal noise, registration errors, and channel decorrelation have been discussed in several papers [1 1-13]. These errors are not removed by the use of ground control points, and the expected magnitude of these errors is dominated by the thermal noise and geometric decorrelation. If we assume a 13 dB signal-to-noise ratio (SNR) at the center of swath and that SNR is proportional to $\cos\theta\, r^{-3}$, where the cosine factor comes from assuming σ^0 follows Lambert's law, for our system parameters we obtain error estimates from thermal noise and baseline decorrelation of 0.8 m vertical and 1.4 m horizontal in the near range (r= 9200 m and θ = 30°) and 2.8 m vertical and 2 m horizontal in the far range (r= 14000 m and θ = 550).

Errors with correlation lengths comparable to the data acquisition path length are generally removable by using ground control points to scale the data and remove tilts and offsets, thus their effects are minimized in the data analysis performed for this paper, but can be significant contributors to the total error when fiducial points arc unavailable. Geometric errors, such as attitude errors and velocity biases, are often of this type, though rubber sheet horizontal distortions can be produced by

shorter-term errors and noise in the position and velocity estimates of the INU, but these errors are generally much smaller than the slowly varying biases.

Azimuth scale errors and azimuth tilts are primarily caused by biases in the along track and vertical velocity estimation of the navigation system. It is our experience that the order of magnitude for these errors are 1 m/see for the along-track velocity and 0.2 m/see for the vertical velocity, consistent with the measured scaling and tilts of the radar DEM. Using a simple geometry assuming broadside (zero Doppler) mapping it is easily seen that an error in the baseline length will introduce range scaling errors, as

$$\sigma_{y,B} = -r\cos\theta\tan(\theta-\alpha)\frac{\sigma_B}{B} \tag{5}$$

illustrating that the horizontal error due to baseline error is proportional to tan(θ – a), Similarly,

$$\sigma_{z,B} = -r\sin\theta\tan(\theta-\alpha)\frac{\sigma_B}{B} \tag{6}$$

shows the vertical error is proportional to – y tan(θ – *a).* If the baseline length knowledge is 1 centimeter, these scaling errors arc about +20 m horizontal and +13 m vertical in the near range and -5 m horizontal and –7 m vertical in the far range. The errors corresponding to a 1 cm baseline error amounts to a horizontal offset and a scale error (approximately 0.4%). These errors are constant and largely removed by the horizontal scaling wc applied. Residual vertical offset and tilt arc removed by the plane removal procedure, except for higher order components of the error. Note that the baseline length errors go to zero when the baseline is orthogonal to the look direction.

An error in baseline orientation (roll angle) corresponds directly to a tilt in the measured surface with respect to the true surface. The short-term accuracy of our measured attitude is -0.01” which corresponds to a vertical error of 0.9 m in near range and 2 m in the far range, while the slowly varying roll bias is significantly larger but can be considered constant over a single run and is therefore efficiently removed by our tilt removal process.

Another distortion results if the absolute phase, that is the number of 2π multiples which must be added to the phase measurements, is determined incorrectly. If the absolute phase is in error by *m* multiples of 2π it can be shown that this results in an error which is equivalent to tilting the measured surface by an amount

$$\sigma_{\theta,m} = \sin^{-1}\left(\frac{\lambda m}{B\cos(\theta-\alpha)}\right) \tag{7}$$

which is approximately proportional 10 $1/\cos(\theta-\alpha)$, i.e. the tilt is range dependent. This introduces both an overall vertical linear error, and a horizontal scaling error, both of which are minimized but not equal to zero when the baseline is orthogonal to the look angle. It is important to note that the tilt is range dependent and cannot be removed completely by a tilt correction.

Finally, horizontal skew can be introduced in the data if it is acquired in a squinted geometry and the along-track velocity is biased, or may be introduced by various approximations within the processor itself. These effects are bit significant in our system.

We can see then that the dominant error sources for data corrected by using comer reflectors are likely to be the random thermal noise/geometrical decorrelation error, and "rubber sheet" medium-term position errors, and that the magnitude of the observed errors is consistent with our expectations, based on our estimates of system performance. Wc note, however, that correlated errors may also be seen in the data, and may be recognized by characteristic banding in range or azimuth. Errors correlated in the range direction arc generally associated with inaccuracies in measurement of aircraft motion leading to motion compensation errors. Errors which arc correlated in azimuth but vary more or less periodically in range we presently believe to be duc to additional scattering centers on the aircraft producing multipath effects which vary as a function of incidcncc angle.

6 . CONCLUSIONS

We have evaluated topographic data acquired by the TOPSAR interferometric SAR systcm and processed with our integrated processing system, Not surprisingly we have found that good horizontal resolution, geometric fidelity and registration are important to achieve good vertical accuracy in rough terrain. We found that registration errors on the order of 2 to 5 meters have a significant impact on the measured DEM errors. In rough terrain the horizontal positioning accuracy must be approximately equal to the required vertical DEM accuracy. Horizontal resolution is probably less critical by a factor 2-3. We also found that processor interpolation and regrinding algorithms are critical.

The measurements reported here are applicable only to relative accuracy as we used comer reflectors to reference our data to WGS-84 coordinates. To achieve the required absolute accuracy directly from the radar measurements would require increased accuracy in the knowledge of aircraft position, velocity and attitude, and the implementation of atmospheric corrections algorithms.

Our experiences from the evaluation experiments we have conducted in both 1991 and 1992 have shown that the performance of interferometric SAR systems in relation to topographic mapping must be split into two separate problems as the sensor system effects should be studied separately from target interaction effects (volume scattering and multi-path on the target). The rough terrain found in the Ft. Irwin area with little or no vegetation has been found well suited for the sensor system evaluation. In addition the availability of state-of-the-art reference DEMs is an important prerequisite for such evaluation experiments.

Carefully planned and executed verification experiments are essential for the calibration of topographic radar mapping systems. Wc note that there arc many parameters to calibrate and, as several of thcm give correlated errors, a correct calibration is not easily achieved. Designing appropriate calibration procedures that will allow the correct determination and/or verification of individual parameters in 3-D mapping radar is a field where more work is clearly needed.

ACKNOWLEDGMENTS

We would like to thank the Army Topographic Engineering Center for providing the reference DEM for this evaluation. In particular we want to acknowledge Raye Norvelle of TEC. We thank JPL's Aircraft Group for installing and operating the TOPSAR radar as well as providing other support. J. Cruz, S, Shaffer, K. Banwart and R. Fatland of JPL deployed the comer reflectors. The research described in this paper was performed at the Jet Propulsion Laboratory, California Institute of Technology, under contract the Advanced Research Project Agency (ARPA).

REFERENCES

[1] A. E. E. Rodgers, and R. P. Ingalls, "Venus: Mapping the surface reflectivity by radar interferometry," Science, 165, pp 797-799, 1969

[2] S. H. Zisk, "A new earth-based radar technique for the measurement of lunar topography," Moon, 4, pp 296-306, 1972a

[3] S. H. Zisk, "Lunar topography: First radar-interferometer measurements of the Alphonsus-Ptolemaeus-Arzachel region," Science, 178, pp 977-980, 1972b

[4] H. C. Rumsey, G. A. Morris, R. R. Green, and R. M. Goldstein, "A radar brightness and altitude image of a portion of Venus," Icarus, 23, pp 1-7, 1974

[51 L, C. Graham, "Synthetic interferometer radar for topographic mapping," Proc. IEEE, 62, pp 763-768, 1974

[6] H. A. Zebker and R. M. Goldstein, "Topographic Mapping From Interferometric Synthetic Aperture Radar Observations," Jour. Geophysical Research, Vol. 91, No. B5, pages 4993-4999, April 10, 1986

[7] R. M. Goldstein, H. A. Zebker and C. Wemcr, "Satellite radar interferometry: two-dimensional phase unwrapping: Radio Science, Vol. 23, No. 4, pages 713-720, July -Aug., 1988

[8] H. A. Zebker, S. N. Madsen, J. Martin, K. B. Wheeler, T. Miller, L. Yunling, G. Alberti, S. Vetrella, and A. Cucci, "The TOPSAR interferometric radar topographic mapping instrument," IEEE Trans. Geoscience and Remote Sensing, vol. 30, No. 5, pp. 933-940, Sept. 1992

[9] S. N. Madsen, H. A. Zebker, and J. Martin, "Topographic Mapping Using Radar Interferometry: Processing Techniques," IEEE Trans. Geoscience and Remote Sensing, vol. 31, No. 1, pp. 246-256, Jan. 1993

[10] S. N. Madsen and H. A. Zebker, "Automated absolute phase retrieval in across-track interferometry," in proceedings of the international geoscience and remote sensing symposium, IGARSS'92, vol. 2, pp. 1582–1 584, 1992

[11] E. R. Rodriguez and J. Martin, 'Theory and design of interferometric synthetic aperture radars," IEE proceedings, vol. 139, pp. **147-159,** April 1992

[12] F, K. Li and R. M. Goldstein, "Studies of multibaseline spaceborne Interferometric synthetic aperture radars," IEEE Trans. Geoscience and Remote Sensing, vol. 28, No. 1, pp. 88-97, Jan. 1990

[13] H. A. Zebker and J. Villasenor, "Decorrelation in interferometric radar echoes," IEEE Trans. Geoscience and Remote Sensing, vol. 30, No. 1, pp. 950-959 Sept. 1992

FIGURE CAPTIONS

Fig. 1. TOPSAR geometry. Radio signals arc transmitted from one antenna and received at both *A1* and *A2.*

Fig. *2.* Map showing the Ft. Irwin area, the location of the TEC reference DEM (blue), and the three radar maps NTC run 1,2, and 3 (red).

Fig. 3. The TEC reference DEM shown as (a) a color image with 400 m between color repeats (16 colors each 25 m) and (b) a shaded relief image.

Fig. *4. NTC* run 1. The radar image brightness is proportional to the backscatter strength, and the elevation, z, is mapped on a color wheel which repeats every 32 m.

Fig. 5. Color map showing the difference between radar and reference DEM heights for run 1.

Fig. 6. Color map showing the difference between radar and reference DEM heights for run 3.

Fig. 7. (a) East-west cut through radar and TEC DEMs; (b) Difference between radar and TEC DEM heights.

Fig. 8. (a) North-south cut through radar and TEC DEMs; (b) Difference between radar and TEC DEM heights.

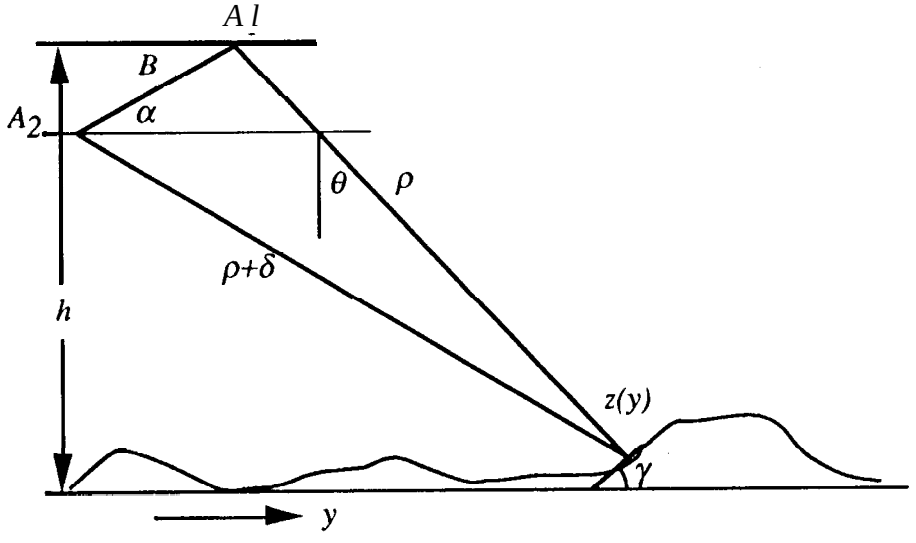

Fig. 1. TOPSAR geometry. Radio signals are transmitted from one antenna and received at both A_1 and A_2.

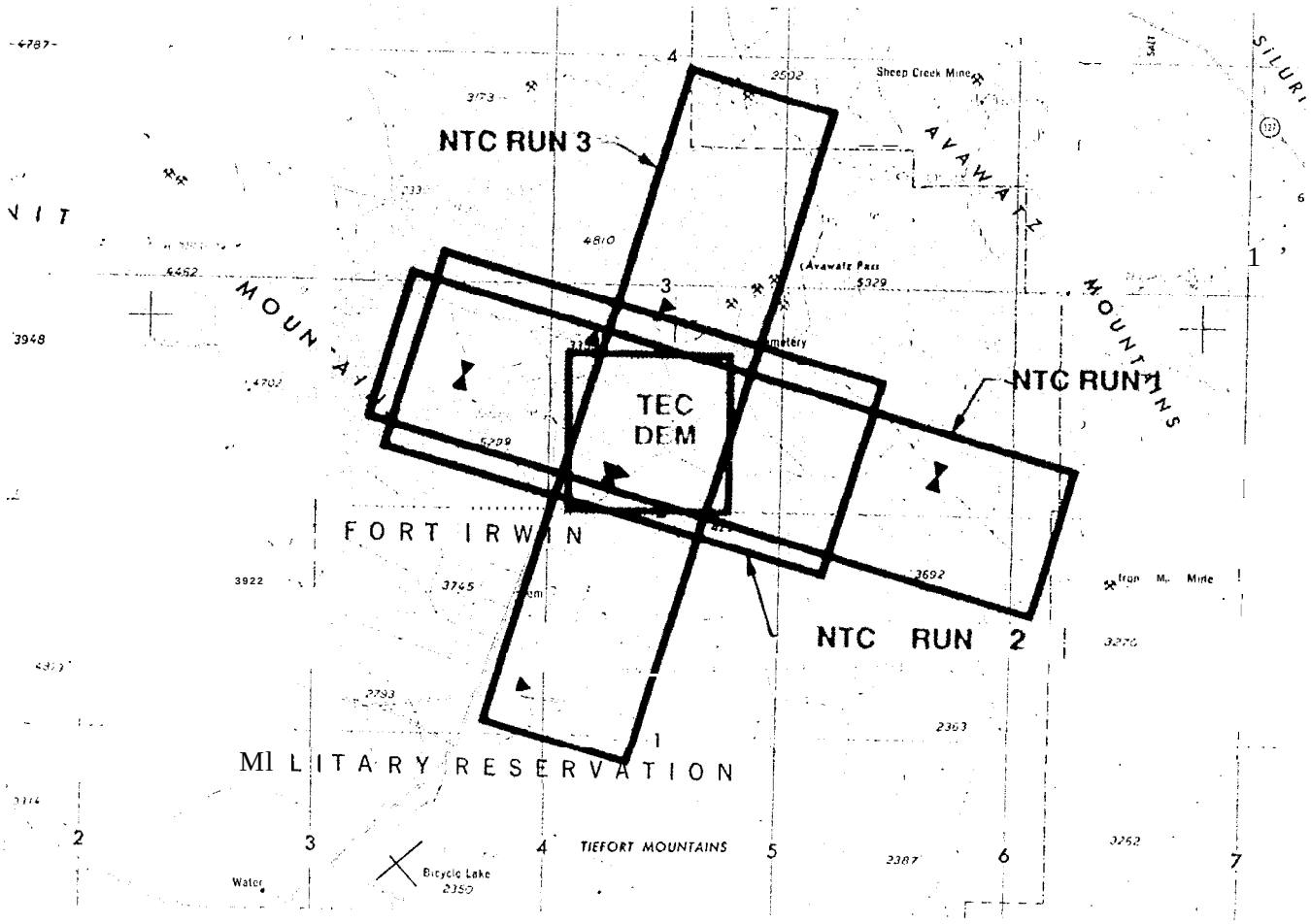

Fig. 2. Map showing the Ft. Irwin area, the location of the TEC reference DEM (blue), and the three radar maps NTC run 1,2, and 3 (red).

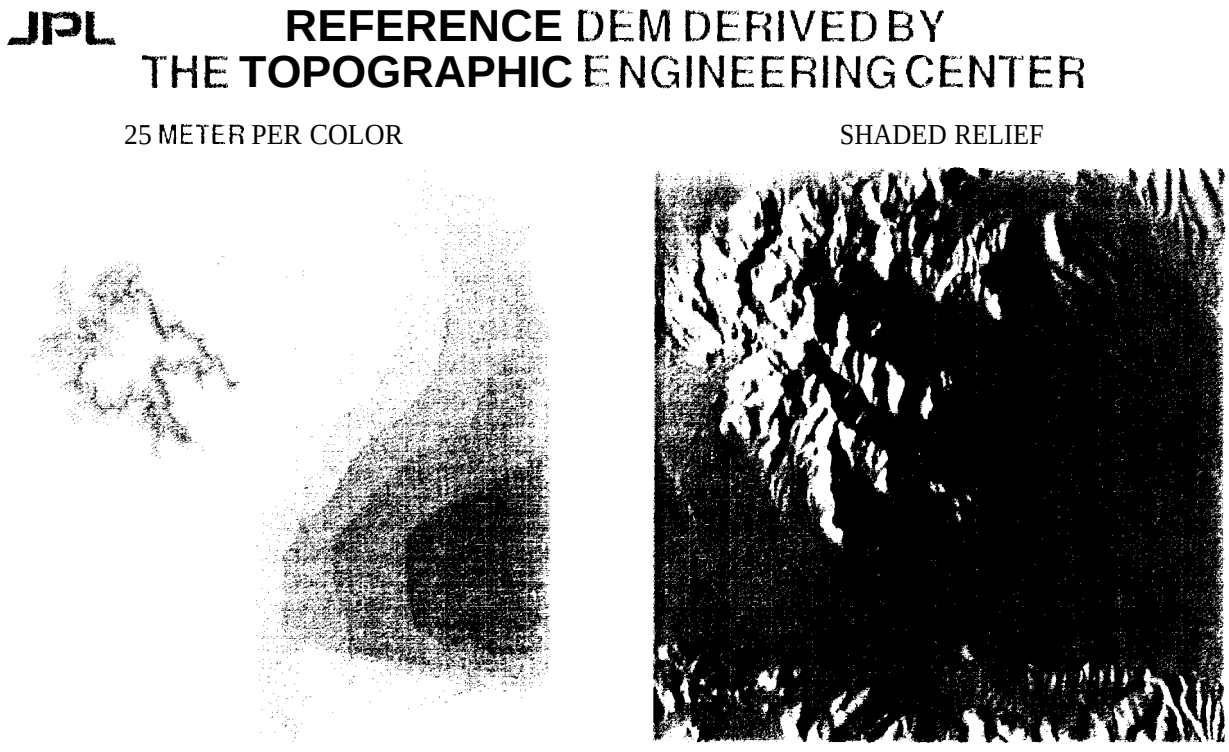

Fig. 3. The TEC reference DEM shown as (a) a color image with 400 m between color repeats (16 colors each 25 m) and (b) a shaded relief image.

JPL TOPSAR DIGITAL ELEVATION MODEL

FT. IRWIN - NTC RUN 1 (6.5 X 30 KM)

BRIGHTNESS = C-BAND BACKSCATTER **COLOR = HEIGHT; 2M/COLOR, 32 M/REPEAT**

Fig. 4. NTC run 1. The radar image brightness is proportional to the backscatter strength, and the elevation, z, is mapped on a color wheel which repeats every 32 m.

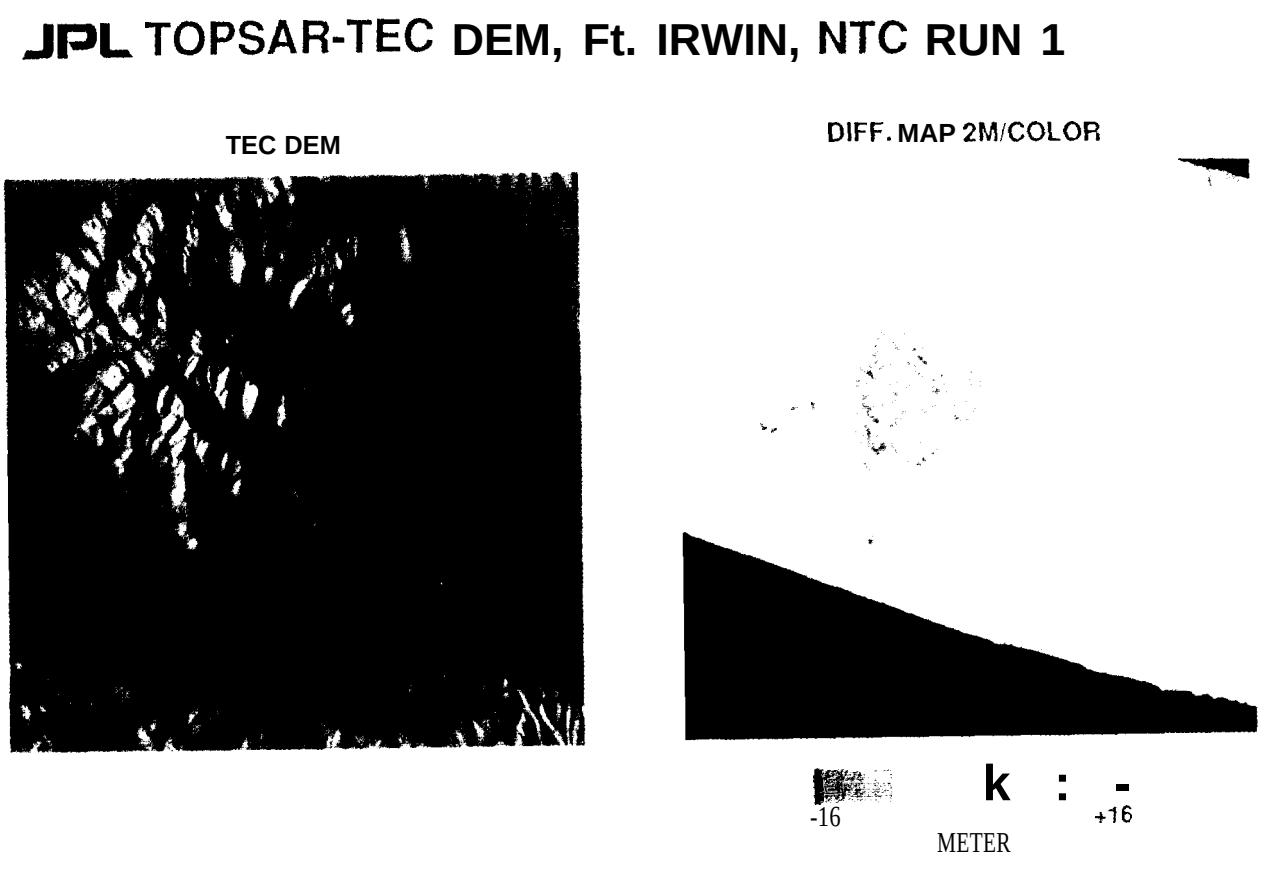

Fig. 5. Color map showing the difference between molar and reference DEM heights for run 1.

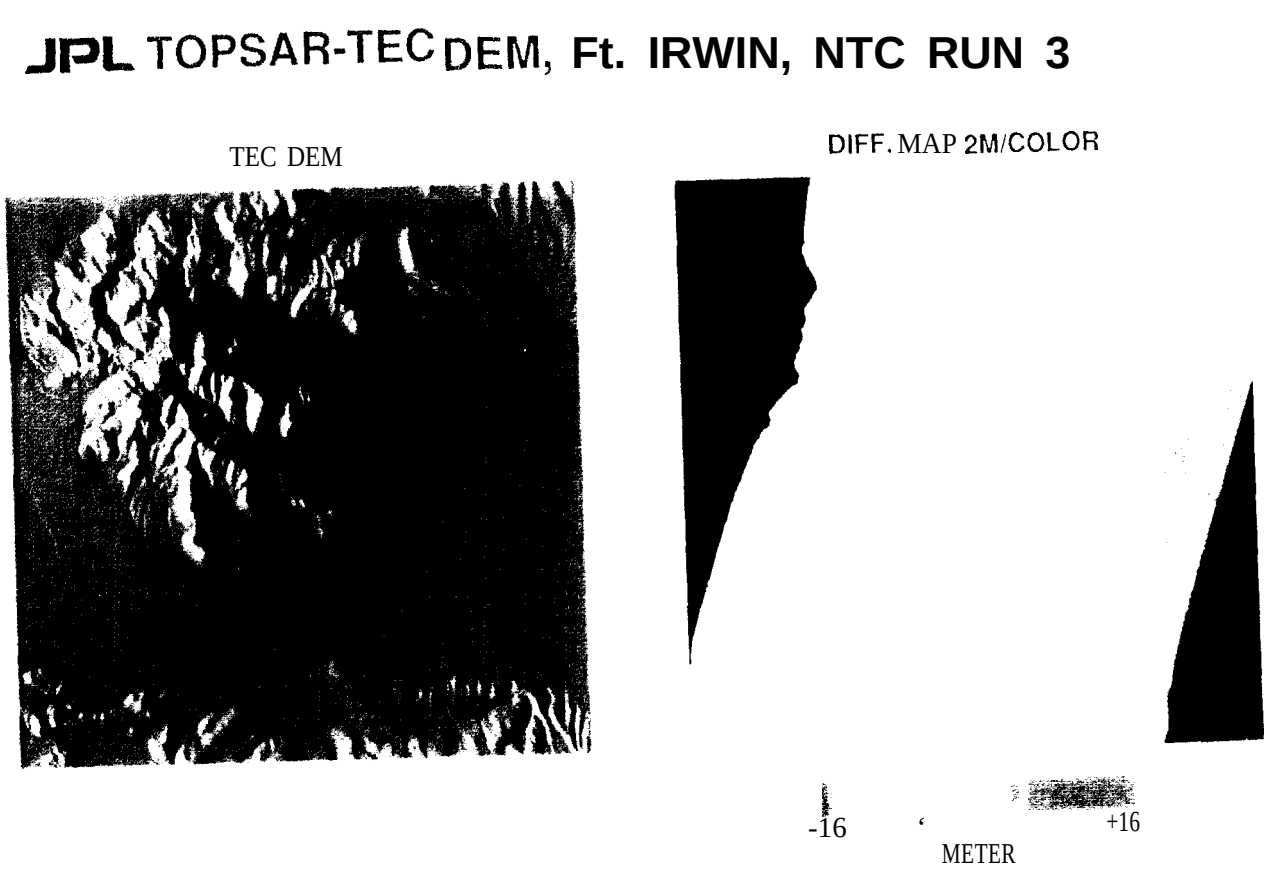

Fig. 6. Color map showing the difference between radar and reference DEM heights for run 3.

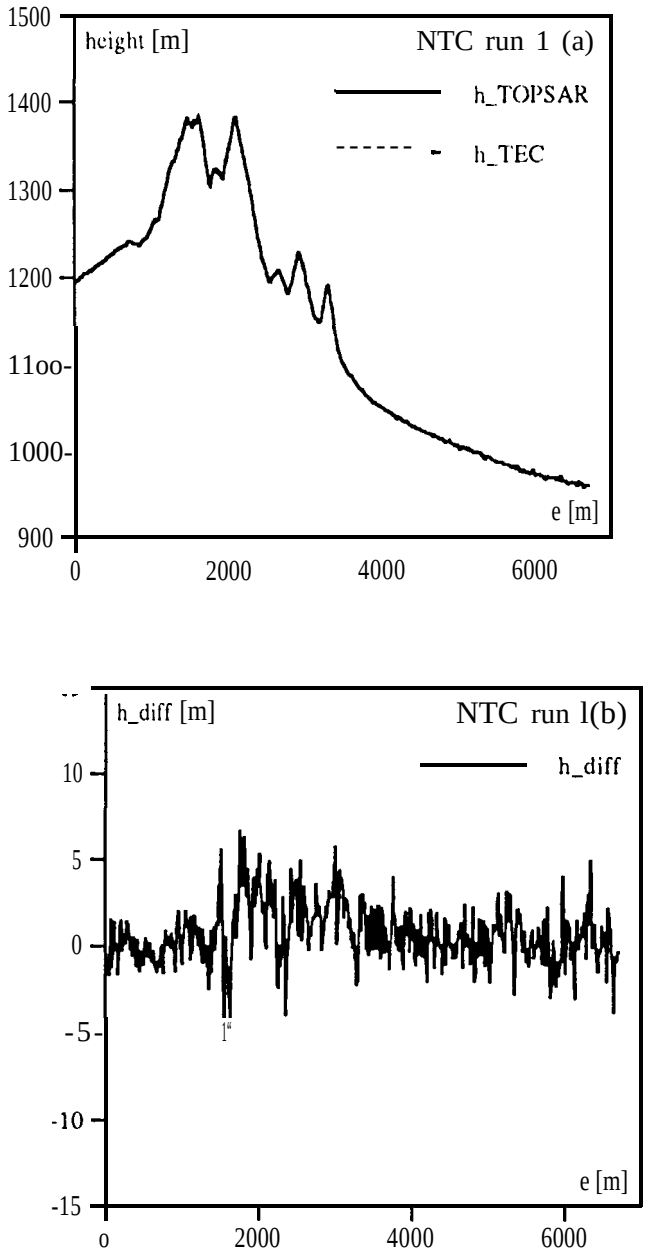

Fig. 7. (a) East-west cut through radar and TEC DEMs; (b) Difference between radar and TEC DEM heights.

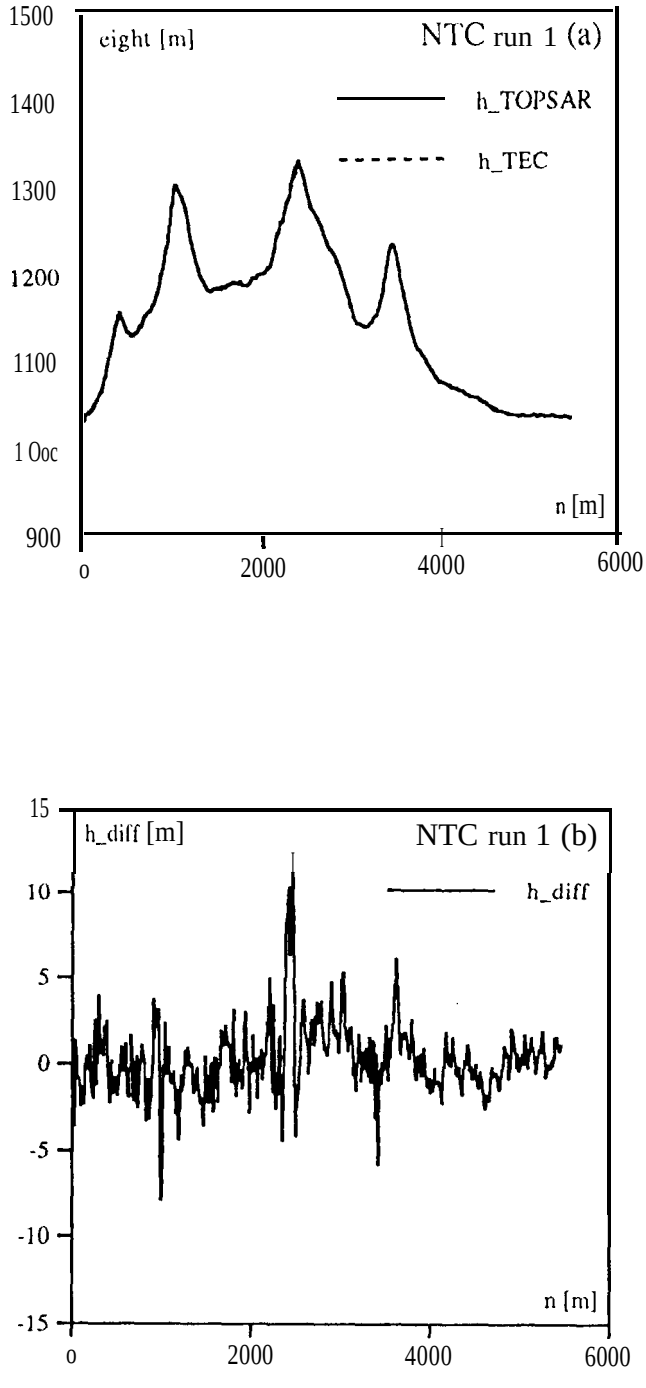

Fig. 8. (a) North-south cut through radar and TEC DEMs; (b) Difference between radar and TEC DEM heights.

TABLE 1.

TOPSAR SYSTEM PARAMETERS (1992)

Radar parameter	*Value*	
Frequency	5.3 GHz	λ = 0.0567 m
Range bandwidth	40 MHz	(or 20 MHz)
Peak transmit power	1000 W	
Pulse repetition rate	2.64/meter	
Antenna length	1.5 m	
Antenna elevation beam width	30°	
Baseline length	2.5 m	
Baseline angle rel. horizontal, ξ	62.8°	
Operating altitude	approx. 9 km	
Look angles	30–55°	
Slant range, near/far	10/15 km	
Processed ground range swath	6.4 km	(or 12.8 km)

TABLE 2.

UTM POSITIONS (WCS 84) OF **CORNER** REFLECTORS AND CORNERS OF REFERENCE **DEM** (10 M HORIZONTAL SPACING)

	Northing [m]	*Easting [m]*	*Elevation [m]*
CR 1A	**3926386.63**	**534761.19**	**1077.43**
CR 1B	3921509.56	543110,69	1031.40
CR 1C	3927778.17	541731.14	998.07
CR 1D	3921843.00	556767.16	934.45
CR 2A	3921868.91	556747.39	935.74
CR 2B	3927763.38	541763.42	998.88
CR 2C	3926428.13	534789.62	1074.44
CR 3A	3929145.24	545001.45	1030.84
CR 3B	3921488.75	543071.5	1032.32
CR 3C	3912145.73	538800.11	706.37
DEM NW	3927050	540230	
DEM NE	3927050	547180	
DEM SE	3919950	547180	
DEM SW	3919950	540230	

TABLE 3

HORIZONTAL TRANSFORMATION PARAMETERS

Parameter	*RUN 1*	*RUN 3*
Azimuth scale factor, λ_x	1,0033	0.9979
Range scale factor, λ_y	1.0025	1.0036
Skew [radians]	-2.2.10-4	$(-2.5.10^{-4})$
Rotation angle [degrees]	73.3	-16.8

TABLE 4

RADAR MINUS REFERENCE DEM, VERTICAL PARAMETERS FOR

CORNER REFLECTOR ALIGNMENT

	NTC RUN 1	*NTC RUN* 3
Parameter	*Entire DEM*	*Entire DEM*
Azimuth tilt [mrad = m/km]	0,44	-0.27
Range tilt [mrad = m/km]	*8.28*	*6.78*
Vertical offset [m]	553.38	571.37
Std. deviation DEM	112.65	112.65
No. of Points in overlap region	391891	389378
Mean cliff. [m]	-0.22	-1.40
Std. deviation cliff. [m]	2.07	3.01
5 sigma pts. rejected:		
Number of points rejected	279	60
Std. deviation cliff. [m]	1.96	2.99

TABLE 5

RADAR MINUS REFERENCE DEM, VERTICAL

PARAMETERS FOR DEM FIT ALIGNMENT

NTC RUN 1	*Entire DEM*	*Flat area*	*Mtn. area*
Std. deviation DEM [m]	112,65	13.70	74.50
No. of Points	391891	10000	10000
Std. deviation cliff. [m]	1.89	1,06	3.31
Mean cliff. [m]	0.00	-0.40	1.30
5 sigma pts. rejected:			
#pts rejected	279	0	114
Std. deviation cliff. [m]	1.76	1.06	2.25

NTC RUN 3	*Entire DEM*	*Flat area*	*Mtn. area*
Std. deviation DEM [m]	112.65	17,85	74.50
No. of Points	389378	10000	10000
Std. deviation cliff. [m]	2.27	1.99	2.15
Mean cliff. [m]	0.00	-0.92	-0.29
5 sigma pts. rejected:			
#pts rejected	228	0	16
Std. deviation cliff. [m]	2.23	1.99	2.02

TABLE 6

HORIZONTAL ERROR SOURCES

Horizontal position errors:	*Error Sources:*
Azimuth scale	Velocity bias (nav. system)
Range scale	Baseline length
	Absolute phase ambiguity
	Slant range calibration
Skew	Velocity bias, processor
Rubber sheet distortion	Mocomp = Nav. + Processor
High frequency across-track	Signal-to-noise-ratio
	Impulse response (ISLR etc.)
	Channel co-registration

TABLE 7

VERTICAL ERROR SOURCES

Vertical errors:	*Error Sources:*
Azimuth tilt	Vertical velocity bias
Range tilt	Attitude biases
	Baseline orientation
	Absolute phase ambiguity
Vertical offset	Nav. system position
Correlated height error	Mocomp = Nav. + Processor
	Multi-path
High frequency random	Signal-to-noise-ratio
	Impulse response (ISLR etc.)
	Channel co-registration